

10467 131 TN 4131

0066916



TECH LIBRARY KAFB, NM

# NATIONAL ADVISORY COMMITTEE FOR AERONAUTICS

TECHNICAL NOTE 4131

TRANSITION-FLIGHT INVESTIGATION OF A  
FOUR-ENGINE-TRANSPORT VERTICAL-TAKE-OFF AIRPLANE MODEL  
UTILIZING A LARGE FLAP AND EXTENSIBLE VANES FOR  
REDIRECTING THE PROPELLER SLIPSTREAM

By Louis P. Tosti

Langley Aeronautical Laboratory  
Langley Field, Va.



Washington

December 1957

TECHNICAL LIBRARY  
AFL 2811



0066916

## TECHNICAL NOTE 4131

TRANSITION-FLIGHT INVESTIGATION OF A  
FOUR-ENGINE-TRANSPORT VERTICAL-TAKE-OFF AIRPLANE MODEL  
UTILIZING A LARGE FLAP AND EXTENSIBLE VANES FOR  
REDIRECTING THE PROPELLER SLIPSTREAM

By Louis P. Tosti

## SUMMARY

An experimental investigation has been conducted to determine the dynamic stability and control characteristics of a four-engine-transport vertical-take-off airplane model in the transition range from hovering to normal forward flight. The model had four propellers located along the wing with the thrust axes essentially parallel to the fuselage axis. In order to produce direct lift for hovering flight the propeller slipstream was deflected downward about  $70^\circ$  by a full-span 65-percent-chord flap and eight retractable vanes arranged above the wing in a cascade relation. All flight tests were made with a pitch damper installed since such a damper had been found to be necessary for satisfactory longitudinal stability in hovering flight in a previous investigation of the hovering condition. The investigation included both flight and static-force tests.

The only serious stability and control difficulty encountered in transition from hovering to forward flight was a divergence in yaw at very low speeds. These yawing divergences were caused by random out-of-trim yawing moments which were sometimes greater than the control forces available. These random changes in yaw trim may be associated with an unsymmetrical breakaway of flow from the upper surface of the flap of a deflected slipstream configuration in which an effort was made to achieve maximum turning angle.

## INTRODUCTION

An investigation has been conducted to determine the dynamic stability and control characteristics of a transport-type four-engine vertical-take-off airplane model. The first phase of the investigation,

which was reported in reference 1, covered the take-off, landing, and hovering flight characteristics of the model. The present investigation consisted of flight tests through the transition from hovering to normal unstalled forward flight and supplementary force tests. The flights were essentially constant-altitude transitions covering a speed range from 0 to about 50 knots.

In order to accomplish transition from hovering to forward flight, a large 0.65 chord main flap was rotated from  $85^\circ$  to  $0^\circ$  and a cascade of auxiliary vanes was rotated to a position perpendicular to the wing chord; the cascade of vanes then folded outwardly as a parallelogram, so as to nest in a recess in the wing. The model was then a conventional monoplane configuration for forward flight.

For control in normal forward flight, the model had conventional elevators, ailerons, and rudder. For hovering flight the controls consisted of a tail jet for pitch and yaw control, differential deflection of the wing control flaps for additional yaw control, and differential change of the pitch of the outboard propeller for roll control.

#### SYMBOLS

The motions of the model and the force-test data are referred to the stability system of axes. Figure 1 shows these axes and the positive direction of the forces, moments, and angular displacements.

The definitions of the symbols used in the present paper are as follows:

$\bar{c}$	mean aerodynamic chord, ft
$C_m$	pitching-moment coefficient referred to the 46 percent chord, $\frac{\text{Pitching moment}}{qS\bar{c}}$
$C_D$	drag coefficient, $\frac{\text{Drag}}{qS}$
$C_L$	lift coefficient, $\frac{\text{Lift}}{qS}$
$q$	dynamic pressure, $\frac{1}{2}\rho V^2$ , lb/sq ft

S	area of wing, sq ft
V	airspeed, ft/sec
X, Y, Z	stability axes
$I_X$	moment of inertia about X-axis, slug-ft <sup>2</sup>
$I_Y$	moment of inertia about Y-axis, slug-ft <sup>2</sup>
$I_Z$	moment of inertia about Z-axis, slug-ft <sup>2</sup>
$F_Y$	lateral force, lb
$F_{Y\beta}$	rate of change of lateral force with sideslip, lb/deg
$M_X$	rolling moment, ft-lb
$M_{X\beta}$	rate of change of rolling moment with sideslip angle, ft-lb/deg
$M_Y$	pitching moment, ft-lb
$M_Z$	yawing moment about the 46-percent-chord station, ft-lb
$M_{Z\beta}$	rate of change of yawing moment with sideslip angle, ft-lb/deg
$i_t$	horizontal-tail incidence (positive in the nose-up direction), deg
$\alpha$	angle of attack of fuselage center line, deg
$\beta_{0.75R}$	propeller blade angle at 0.75 radius, deg
$\beta$	sideslip angle, deg
$\gamma$	angle between vane supports and lateral axis during retraction, deg
$\delta$	main-flap deflection, deg
$\delta_e$	elevator deflection, deg
$\delta_f$	deflection of control flaps on wing, deg

$\delta_r$	rudder deflection, deg
$\theta$	angle of pitch of the fuselage relative to horizontal, deg
$\phi$	roll angle, deg
$\psi$	angle of yaw, deg
$\epsilon$	downwash angle, deg
$\rho$	density, slugs/cu ft

#### APPARATUS AND MODEL

The flight investigation was conducted by the Langley Free-Flight Tunnel Section in the 30- by 60-foot test section of the Langley full-scale tunnel. The test setup is illustrated in figure 2. The sketch shows the pitch pilot, the model power operator, the flap and vanes operator, and the safety cable operator on a balcony at the side of the test section. The roll pilot was in an enclosure in the lower rear part of the test section, and the yaw pilot was at the top rear of the test section. The tunnel operator, who regulated the tunnel airspeed, was in the control room below the balcony. The three pilots were located at positions which gave them good vantage points for observing and controlling the particular phase of the motion of the model with which they were concerned. Motion-picture records were obtained with fixed cameras mounted near the pitch and yaw pilots.

The power for the model propulsion motor, the tilting motor for the main flap and vanes, and the electric control solenoids was supplied through wires; and the air for the control actuators was supplied through plastic tubes. These wires and tubes were suspended from above and taped to a safety cable (1/16-inch braided aircraft cable) from a point about 15 feet above the model down to the model. The safety cable, which was attached to the top of the model near the center of gravity, was used to prevent crashes in the event of a power or control failure or in the event that the pilots lost control of the model. During flight the cable was kept slack, so that it did not appreciably influence the motions of the model.

The flying model used in the present investigation had four propellers with the thrust axes at an incidence of  $5^\circ$  relative to the fuselage axis. The propellers were located along the wing span so that the turning vanes and most of the wing were immersed in the slipstream. The wing had a full-span plain flap of about 65 percent chord which was deflected about  $85^\circ$  for hovering flight. The trailing portion of the

flap was hinged as a control flap and had a chord of 25 percent of the wing chord. Eight evenly spaced turning vanes were located above the wing in a cascade relation to turn the slipstream downward to produce direct lift for hovering flight. The model was the same one used in the investigation of reference 1 with the following exceptions: the wing incidence relative to the fuselage was increased to  $5^\circ$ , the overall weight was increased because of the additional equipment necessary to permit transition from hovering to forward flight, and the control system was revised. Photographs of the model are presented in figure 3. A three-view drawing showing some of the more important dimensions of the model is presented in figure 4 and the characteristics are listed in table I. Details of the wing and vane arrangement are given in reference 1. The model power was supplied by a 10-horsepower electric motor which drove the four propellers by means of shafting and right-angle gear boxes. The speed of the motor was changed to vary the thrust of the propellers. In order to accomplish transition from hovering to forward flight, the main flap rotated from  $85^\circ$  to  $0^\circ$  and the cascade of auxiliary vanes rotated  $42.5^\circ$  to a position perpendicular to the wing-chord plane; the cascade of vanes then folded outwardly as a parallelogram so as to nest in a recess in the wing. The model was then a conventional monoplane configuration for forward flight as shown by the photograph in figure 3(b). This retraction system was selected on the basis of mechanical simplicity for a small-scale dynamic model and not on the basis of an optimum arrangement for a full-scale airplane. There was almost no movement of the center of gravity of the model with the movement of the main flap and vanes through the flight range.

Pitch control in hovering and low-speed flight was obtained by deflecting a compressed-air tail jet to produce a maximum pitching moment of about  $\pm 12$  foot-pounds. In order to save weight in the model, the elevator and the tail jet were operated by the same control actuator so that both controls operated during the entire flight. The elevator deflection used was  $\pm 13^\circ$  from the trim position.

Yaw control in hovering and low-speed flight was obtained partly by deflecting a compressed-air tail jet to produce a maximum yawing moment of about  $\pm 6$  foot-pounds and partly by deflecting the control flaps differentially  $\pm 15^\circ$ . The rudder was operated by the same actuator as the yaw jet, and could not be switched out of the yaw-control circuit, so it operated throughout the flight range with a deflection of  $\pm 8^\circ$ . Shortly after the transition to forward flight started, at an airspeed of about 15 knots, the control flaps were switched out of the yaw-control circuit because they gave unwanted rolling moments.

Roll control in hovering and low-speed flight was obtained by differentially varying the pitch of the outboard propellers  $\pm 2^\circ$ . At a speed of about 35 knots the roll pilot switched the control flaps into the roll-control circuit as ailerons but the control of the propellers

was not switched out of the roll-control circuit at any time throughout the transition range.

All controls, except pitch control, were deflected by flicker-type (full on or full off) pneumatic actuators which were remotely operated by the pilots. These control actuators were equipped with integrating-type trimmers which trimmed the controls a small amount in the direction that the controls were moved each time a control movement was applied. With actuators of this type, the model became accurately trimmed after flying a short time in a given flight condition.

A rate-sensitive artificial stabilizing device was used in the flight tests to increase the damping of the pitching motions since this device had been found to be very beneficial in hovering flight as reported in reference 1. This pitch damper consisted of a rate gyroscope which, in response to rate of pitch, provided signals to a proportional control actuator which moved the control to oppose the pitching motion. This proportional control actuator had an override mechanism attached to it so that a manual pitch control would override the signal from the gyroscope and give full pitch control in the desired direction.

#### FLIGHT TEST TECHNIQUE

The test technique is best explained by describing a typical flight. The model hangs on the safety cable and the power to the model and to the tunnel-drive motors is turned on. As the airspeed is increased, the attitude of the fuselage is kept essentially horizontal and the main flap and vanes are rotated, as described previously, and the model power is adjusted to provide the necessary thrust to balance the drag of the model. At an airspeed of about 15 knots the yaw pilot switches out the control flap and uses only the tail jet and rudder controls for the remainder of the flight. At an airspeed of about 35 knots the roll pilot switches the control flaps into the roll-control circuit as ailerons. The power and controls are operated to keep the model as near the center of the test section as possible. Throughout the flight the pilots observe the stability and control characteristics of the model and later report their qualitative observations of these characteristics. Separate pilots are used to control the model in pitch, roll, and yaw since it had been found that if a single pilot operates all three controls, he is so busy controlling the model that he has difficulty in ascertaining the true stability and control characteristics of the model about its various axes. The flight is terminated by gradually taking up the slack in the safety cable while reducing the power to the model and the tunnel airspeed.

## TESTS

The flight tests were made through the transition range from hovering to a forward-flight speed of about 50 knots. If the model is considered as a 1/10-scale model of an airplane, the highest speed reached in the tests corresponds to about 160 knots full scale. The flight-test results were obtained in the form of pilots' observations and opinions of the behavior of the model, motion-picture records of the motions of the model, and time histories of the tests made from the motion-picture records.

During the flight tests the stability and control characteristics were studied for two center-of-gravity locations: 39 and 46 percent mean aerodynamic chord. The weight and the moments of inertia of the model as given in table I are for a center of gravity at 46 percent mean aerodynamic chord. The center of gravity was moved forward to 39 percent mean aerodynamic chord by adding 2 pounds of lead in the nose.

Force tests were made in the Langley free-flight tunnel to measure the static stability of the model with the center of gravity at 46 percent mean aerodynamic chord and to determine the effectiveness of the aerodynamic controls. In addition to tests of the control system used for the transition flights, the investigation also included measurements of the effectiveness of the control flaps as a pitch control, since that was the pitch-control system used in the hovering tests of reference 1. Most of the tests were run at about one-half rated speed of the model motor with the tunnel airspeed adjusted to produce zero net drag on the model for the particular test condition.

Since conventional aerodynamic coefficients lose their significance and tend to become infinite as the airspeed approaches zero during the transition, the results of the force tests for the transition range are presented in dimensional form. All of the forces and moments have been scaled up to correspond to the actual forces and moments experienced on the model when flying at a weight of 60.5 pounds. This scaling up was accomplished by multiplying all of the forces and moments measured for a particular main-flap angle by the factor required to scale the lift up to 60.5 pounds for the case of fuselage angle of attack of  $10^\circ$  and neutral controls at the same main-flap setting.

No tunnel wall or blockage corrections have been applied to the force-test data. It is expected that these corrections would be relatively large for the low-speed part of the transition range, since the model was rather large in comparison to the 12-foot octagonal-shaped test section of the free-flight tunnel where the force tests were made.

The force tests for the transition range at various deflections of the main flap and turning vanes included a determination of the static



longitudinal stability of angle of attack, the effectiveness of all of the aerodynamic controls (wing control flaps, elevator, rudder, and propeller pitch), and the variation of lift, drag, and pitch during retraction of the turning vanes. The force tests in the normal forward-flight range consisted of a determination of longitudinal stability for various values of thrust corresponding to trim or zero net drag at various angles of attack.

## RESULTS AND DISCUSSION

A motion-picture film supplement to this paper has been prepared and is available on loan. A request card form and a description of the film will be found at the back of this paper, on the page immediately preceding the abstract and index pages.

### Longitudinal Stability and Control

Transition from hovering to forward flight.- The transition from hovering to normal forward flight was accomplished successfully for two center-of-gravity positions - 39 and 46 percent mean aerodynamic chord. Figures 5 and 6 show time histories of typical flights made at each of these center-of-gravity positions. The pilot observed that, when the center of gravity was at 39 percent mean aerodynamic chord, the transition could be performed easily from the standpoint of longitudinal stability and control. When the center of gravity was at 46 percent mean aerodynamic chord, however, the longitudinal control was marginal. The model experienced a large nose-up change in trim as the speed began to increase from the hovering condition, and the control available was barely sufficient to trim the model in the low-speed range. This point is illustrated by the force-test data of figure 7, which are directly applicable since all the force-test data are referred to the 46-percent-chord center-of-gravity location. These data show that, with the elevator deflected down  $20^\circ$ , there was still a nose-up pitching moment of about 10 to 12 foot-pounds which had to be trimmed out by the tail jet over the range of main-flap angles from  $25^\circ$  to  $65^\circ$ . Inasmuch as the tail jet could produce a moment of only 12 foot-pounds, all the available pitch control was required for trim with this center-of-gravity location. It would not be possible, therefore, to perform the transition with the center of gravity at any more rearward location, since the nose-up pitching moments would then exceed the capabilities of the pitch-control system.

The center of gravity at 46 percent mean aerodynamic chord was the position at which the model required no trim pitching moment from the tail jet for hovering flight. Because this center-of-gravity position

was the most rearward at which the transition could be performed, the range of allowable center-of-gravity positions was limited to one-half the range that could be trimmed in hovering flight. No attempt was made to determine the most forward center-of-gravity position for which the model could be flown in both the hovering and transition ranges of flight. It seems certain, however, that the forward limit of the center-of-gravity range would be established by the requirements of longitudinal trim and control for hovering flight. Flight tests of the tilting-wing vertical-take-off transport model of reference 2, which was very similar to the present model, showed that this model could be flown successfully in hovering flight with the center of gravity 12 percent chord forward of the position required for neutral trim. Inasmuch as this tilting-wing model had the same tail jet control and had a very similar stability problem with an unstable pitching oscillation in hovering flight (see refs. 1 and 3), it seems likely that the present model could also be flown successfully with the center of gravity located 12 percent mean aerodynamic chord ahead of the position for neutral trim in hovering flight and would therefore have a total allowable center-of-gravity range of 12 percent mean aerodynamic chord.

The control flaps had been used as the pitch control in the hovering tests of reference 1; however, since a jet had been installed at the tail to give a more powerful yaw control than had been available in the hovering tests, it was convenient to make it serve also for pitch control. No attempt was made, therefore, to make the transition with the control flaps instead of the tail jet used as the hovering pitch control. The force-test data in figure 8 show, however, that the control flaps afford a much weaker pitch control than the tail jet and would have been completely inadequate for trimming out the large nose-up pitching moments that were encountered in the low-speed part of the transition range corresponding to main-flap deflections of  $40^\circ$  to  $70^\circ$ .

The power required to fly the model was observed to be greatest for hovering flight. It decreased rapidly as the speed was increased during the transition, then reached a minimum, and finally increased.

After a transition from hovering to normal unstalled forward flight had been completed by rotating the main flap to  $0^\circ$  and by turning the cascade of auxiliary vanes to a position in which the vane supports were perpendicular to the wing-chord plane, the vanes were retracted as explained in the description of the model. The flight tests indicated that during the retraction of the vanes it was necessary to increase gradually the angle of attack and the power required to fly the model in steady level flight until the vanes were almost completely retracted; the power then had to be decreased during the remainder of the retraction of the vanes. The pilots preferred to have the vanes retracted slowly since it permitted better coordination of pitch control and power changes and thus resulted in smoother flights than was possible when the

vanes were retracted quickly. The force-test data in figure 9 show the variation of lift, drag, and pitching moment with vane position during retraction of the vanes for a constant angle of attack. These data show no abrupt change in any of the longitudinal characteristics of the model when the vanes were retracted. A gradual reduction in lift occurred as the vanes were retracted to the  $10^\circ$  position which had to be counteracted by an increase in angle of attack during the flight tests, since the tunnel airspeed could not readily be increased to permit achievement of greater lift by increasing speed. The tests also show a gradual reduction in drag, which was evidently offset during the flight tests by the increase in drag caused by increasing angle of attack, inasmuch as it was found necessary to increase power during most of the time the vanes were being retracted. The force-test data also show a slight increase in lift with a further decrease in drag as the vanes are retracted from  $10^\circ$  to  $0^\circ$ , a result which agrees well with the results of the flight tests.

The variation with forward speed of main-flap deflection required for zero net drag as obtained from the force tests is shown in figure 10. An unexpected result was encountered in tests at main-flap deflections from  $85^\circ$  to  $70^\circ$  in that two trim speeds were obtained for a given main-flap deflection. This effect is also illustrated in figure 11, which shows the variation of drag with forward speed for a main-flap angle of  $85^\circ$ . This effect was believed to be caused by separation of air flow from the upper (or rearward) surface of the main flaps and failure of the flow to turn through as great an angle when the speed was increased beyond a value of 9 knots. As the speed was further increased, the flow stabilized in a new pattern and gave a second stable trim point at 17 knots. No effect of the double trim point on the longitudinal behavior of the model during flight tests was noted. It is believed, however, that this separation of flow was responsible for some of the directional trim problems to be discussed subsequently.

The static longitudinal stability of the model can be determined from the data of figure 12 by comparison of the pitching-moment curves for the three fuselage angles of attack at any given main-flap deflection. Such an analysis indicates that the model was unstable in the low-speed transition range at main-flap deflections from  $85^\circ$  to  $40^\circ$ , and was stable for the higher speeds (smaller main-flap deflections). During the flight tests there was no evidence of any longitudinal instability at these lower speeds. Apparently, the angle-of-attack instability was offset by the pronounced speed stability that is generally characteristic of propeller-driven airplanes. It is also likely that, even if the model had a divergent tendency in this speed range, the rates of divergence were very low because of the low airspeed. Since the model was changing trim during the transition and the pilot was expecting to use continuous control on the model, he might not have noticed a low rate of divergence.

Forward flight.- In the normal forward-flight condition the model flew very smoothly and was easy to fly. This configuration flew much more steadily than the tilting-wing model of references 2 and 4 - perhaps because of the pitch damper or perhaps because of very high static longitudinal stability. The longitudinal stability characteristics with the model trimmed in drag at various fuselage angles of attack for the normal forward-flight condition are presented in figure 13. These results show that the model was very stable throughout the normal flight range with the power settings required for steady level flight. In fact, the data show that the aerodynamic center of the model was about 45 percent mean aerodynamic chord behind the center of gravity or was at about 90 percent mean aerodynamic chord. Additional tests were made to determine the reason for this very high stability. The data of figure 14 show that sealing the slots in the wing, into which the vanes retract, gave the model an appreciable increase in lift-curve slope from 0.059 to 0.097 with little change in the variation of pitching moment with angle of attack. The variation of pitching-moment coefficient with lift coefficient, therefore, is unduly high with the wing slot unsealed because of the low lift-curve slope of the wing. The low lift-curve slope of the wing with the slot unsealed probably results from the fact that air going up through the slot "spoils" the lift and that this spoiling effect increases with angle of attack, since the leakage increases as the pressure differential between the upper and lower surfaces increases. The data indicate that sealing the wing slots moved aerodynamic center of the model forward from about 90 to 70 percent mean aerodynamic chord. Analysis of the data in figure 15 also indicates an unusually small rate of change of downwash at the tail. Normally, the variation of downwash angle with angle of attack  $d\epsilon/d\alpha$  is about 0.5, whereas the variation was about 0.2 on this model as flown with the slots in the wing unsealed and 0.3 with the slots sealed. This low value of  $d\epsilon/d\alpha$ , together with the high aspect ratio of the tail, resulted in a high tail effectiveness; and the combination of low lift-curve slope of the wing and high tail effectiveness resulted in the very high static stability of the model.

#### Lateral Stability and Control

Hovering and low-speed flight.- In general, the lateral stability and control characteristics of the model were satisfactory except for large random yawing moments in hovering and at low speeds, which sometimes became larger than the control moments and caused the model to diverge uncontrollably. At times, when the air was first started in the tunnel, the model would turn tail into the wind and could not be turned around again by use of the yaw controls.

In the hovering phase of flight reported in reference 1, the model was thought to have a weak yaw control because it frequently diverged in

yaw despite the application of full opposite yaw control. It was therefore decided to change the control system for the transition tests by using a tail jet to give a more positive and powerful yaw control. In the present investigation, with the revised control system, however, the model continued to diverge in yaw during hovering and low-speed forward-flight conditions. The original yaw control system (differential deflection of the wing control flaps) was put back in the model and used in conjunction with the tail jet. Although the flaps improved the yaw control somewhat, they did not correct the trouble, and the model still diverged uncontrollably in yaw in more than one-half the flights attempted.

When the force tests were made after the flight-test program was completed, the reasons for the yawing instability became apparent. The data in figure 16 showed that the yawing moments produced by the control flaps, which had seemed so inadequate in the hovering tests reported in reference 1, were actually greater than the yawing moment required for flying the tilting-wing model of references 2 to 4 satisfactorily. It was apparent therefore that the difficulties in yaw control of the present model must be attributed to the fact that the deflected slipstream model was more subject to yaw disturbances than the tilting-wing model, and that a much stronger control in yaw would be required for the model. A clue to the difficulty was offered in the results of force tests for model drag against forward speed with the model in the hovering configuration (fig. 11). Two drag trim points were noted at low forward speeds, which indicated a flow separation from the main flap. It seems likely that gusts caused by tunnel turbulence or by random slipstream recirculation tend to make the air flow break away on one side or another of the wing of the present model; thus large yawing moments are encountered during hovering and at very low forward speeds. Such a breakaway of flow would not be experienced with the tilting wing model, inasmuch as the wing was operating near zero lift in hovering and at very low forward speeds. A rough qualitative check of the effect of gusts was made with the deflected slipstream model in the hovering attitude on a strain-gage balance which was connected to a continuous recorder. A 2-foot-square piece of plywood was used to fan the air by hand in front of the model at various rates of speed. The yawing-moment recorder needle went off scale even at some of the lower-speed gusts so that yawing moments much greater than the control moments were indicated. The difficulty experienced in yaw control therefore seems to be related to the particular configuration of the model but might also be expected to some degree on other vertical-take-off airplanes utilizing the deflected-slipstream principle.

Transition and forward flight.- For those flight tests in which the model did not diverge in yaw at low speeds, the model was flown through the transition range from hovering to forward flight quite successfully. At the higher transitional speeds, with either of the two center-of-gravity positions that were used, the model did not seem to have the

Dutch-roll stability problems experienced with the tilting-wing airplane model of reference 4 and seemed to fly much more smoothly than the tilting-wing model.

The static lateral stability characteristics of the model are presented in figure 17. The slopes of these curves, taken at angles of sideslip between  $\pm 10^\circ$  are presented in figure 18. The yawing moment due to sideslip and rolling moment due to sideslip show large variations throughout the transition range. In the flight tests, however, there was no evidence of any pronounced change in the stability of the model. Apparently, the rates of divergence, if any, were small and were masked by the changes in trim required during the transition and by gust disturbances.

The force-test data on the effectiveness of the lateral controls are presented in figures 16, 19, and 20 to provide an indication of the effectiveness of the various types of control through the transition range.

#### SUMMARY OF RESULTS

Results have been presented from an investigation of the dynamic stability and control characteristics of a vertical-take-off transport-airplane model in transition from hovering to forward flight. The only serious stability and control difficulty encountered in transition from hovering to forward flight was a divergence in yaw at very low speeds. These yawing divergences were caused by random out-of-trim yawing moments which were sometimes greater than the control forces available. These random changes in yaw trim seem to be related to the particular wing-flap-vane system used on the model and might also be expected to be experienced to some degree on other deflected-slipstream vertical-takeoff airplane configurations. Successful transitions were accomplished for a range of center-of-gravity positions of 7 percent mean aerodynamic chord. No attempt was made to determine how large a range of allowable center of gravity was possible, but analysis indicated that a range of about 12 percent mean aerodynamic chord would have been permissible for this particular model.

Langley Aeronautical Laboratory,  
National Advisory Committee for Aeronautics,  
Langley Field, Va., September 11, 1957.

## REFERENCES

1. Tosti, Louis P., and Davenport, Edwin E.: Hovering Flight Tests of a Four-Engine-Transport Vertical Take-Off Airplane Model Utilizing a Large Flap and Extensible Vanes for Redirecting the Propeller Slipstream. NACA TN 3440, 1955.
2. Lovell, Powell M., Jr., and Parlett, Lysle P.: Flight Tests of a Model of a High-Wing Transport Vertical-Take-Off Airplane With Tilting Wing and Propellers and With Jet Controls at the Rear of the Fuselage for Pitch and Yaw Control. NACA TN 3912, 1957.
3. Lovell, Powell M., Jr., and Parlett, Lysle P.: Hovering Flight Tests of a Transport Vertical-Take-Off Airplane With Tilting Wing and Propellers. NACA TN 3630, 1956.
4. Lovell, Powell M., Jr., and Parlett, Lysle P.: Transition Flight Tests of a Model of a Low-Wing Transport Vertical-Take-Off Airplane With Tilting Wing and Propellers. NACA TN 3745, 1956.

TABLE I.- CHARACTERISTICS OF MODEL

Weight, lb . . . . .	60.5
$I_x$ , slug-ft <sup>2</sup> . . . . .	3.01
$I_y$ , slug-ft <sup>2</sup> . . . . .	3.10
$I_z$ , slug-ft <sup>2</sup> . . . . .	5.88
Fuselage length, in. . . . .	85.3
Propellers (two blades each):	
Diameter, in. . . . .	20
Solidity (each propeller) . . . . .	0.079
Wing:	
Sweepback (leading edge), deg . . . . .	0
Airfoil section . . . . .	NACA 0018
Aspect ratio . . . . .	7.13
Tip chord, in. . . . .	10.8
Root chord (at center line), in. . . . .	15.0
Taper ratio . . . . .	0.72
Area (total to center line), sq in. . . . .	1186.8
Span, in. . . . .	92
Mean aerodynamic chord, in. . . . .	13.03
Control-flap hinge line, percent chord . . . . .	75
Dihedral angle, deg . . . . .	0
Leading edge to main flap pivot, in. . . . .	4.5
Vertical tail:	
Sweepback (leading edge), deg . . . . .	5.0
Airfoil section . . . . .	NACA 0009
Aspect ratio . . . . .	1.94
Tip chord, in. . . . .	7.54
Root chord (at center line), in. . . . .	11.12
Taper ratio . . . . .	0.68
Area (total to center line - excluding dorsal area), sq in. . . . .	169.1
Span (from fuselage center line), in. . . . .	18.125
Mean aerodynamic chord, in. . . . .	9.45
Rudder (hinge line perpendicular to fuselage center line):	
Tip chord, in. . . . .	2.5
Root chord, in. . . . .	4.05
Span, in. . . . .	14.03
Horizontal tail:	
Sweepback (leading edge), deg . . . . .	7.3
Airfoil section . . . . .	NACA 0009
Aspect ratio . . . . .	6.17
Tip chord, in. . . . .	4.6
Root chord (at center line), in. . . . .	8.62
Taper ratio . . . . .	0.53
Area (total to center line), sq in. . . . .	269.4
Span, in. . . . .	40.75
Mean aerodynamic chord, in. . . . .	6.81
Elevator (hinge line perpendicular to fuselage center line):	
Tip chord, in. . . . .	2.13
Root chord, in. . . . .	3.30
Span (each), in. . . . .	16.94
Maximum thrust of tail jet for control:	
Normal force (to give pitching moment), lb . . . . .	±2.7
Side force (to give yawing moment), lb . . . . .	±1.3



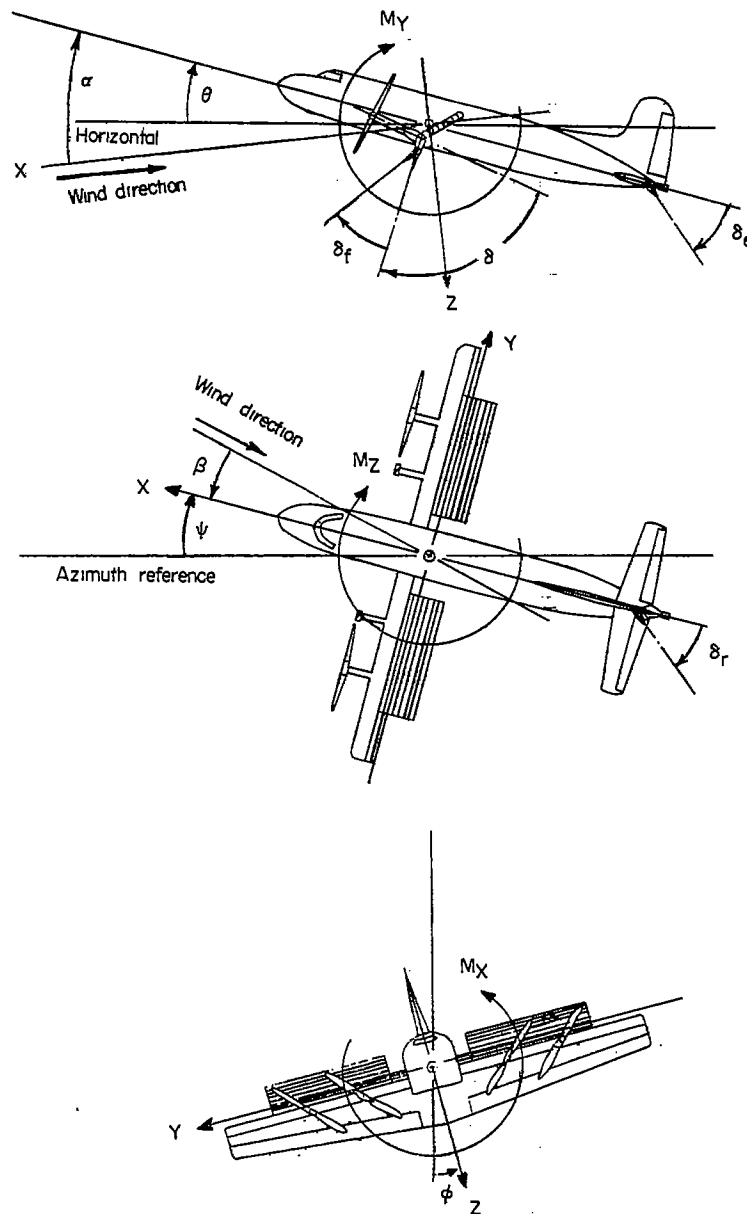


Figure 1.- The stability system of axes. Arrows indicate positive directions of moments, forces, and control deflections. This system of axes is defined as an orthogonal system having the origin at the center of gravity and in which the Z-axis is in the plane of symmetry and perpendicular to the relative wind, the X-axis is in the plane of symmetry and perpendicular to the Z-axis, and the Y-axis is perpendicular to the plane of symmetry.

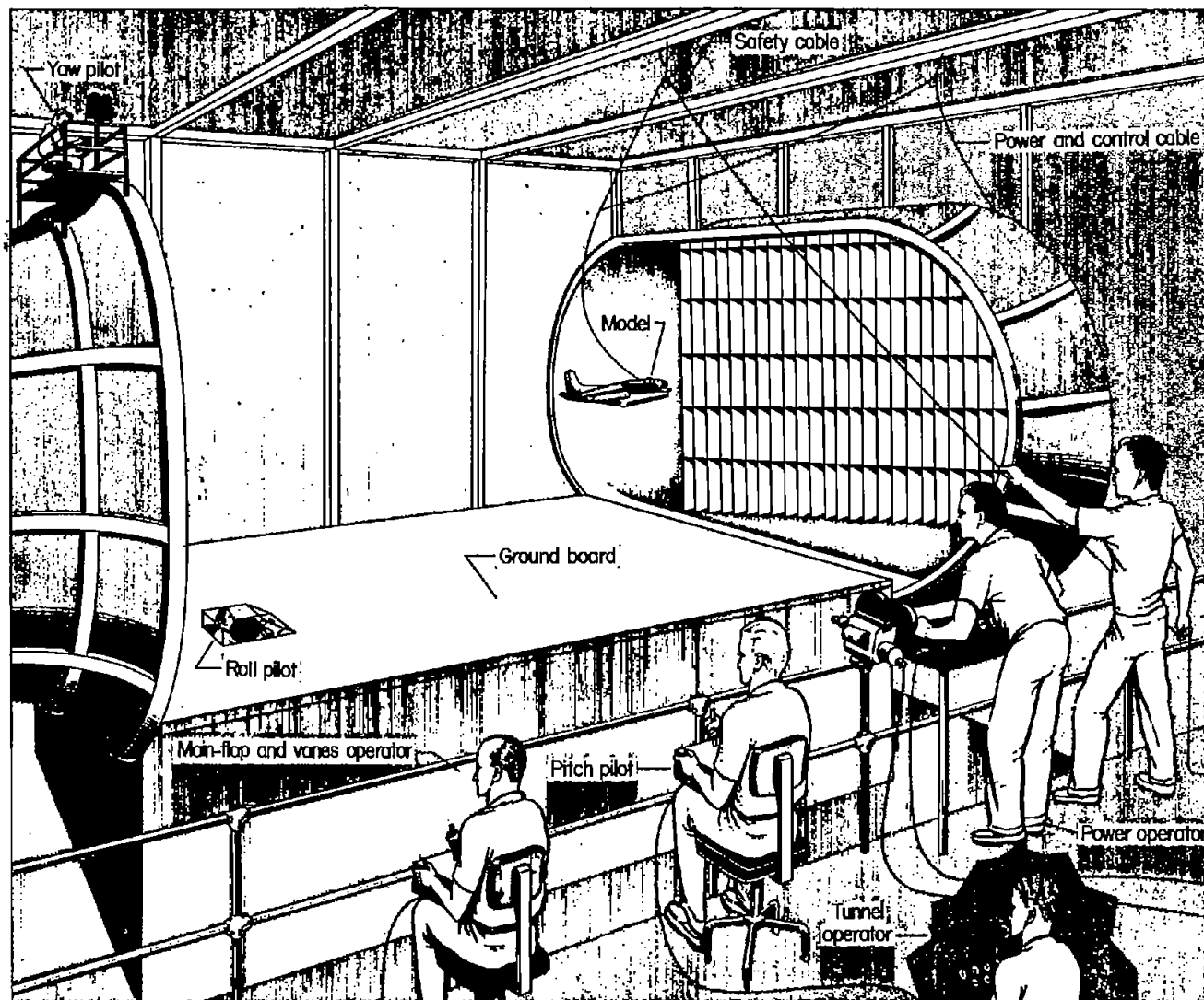
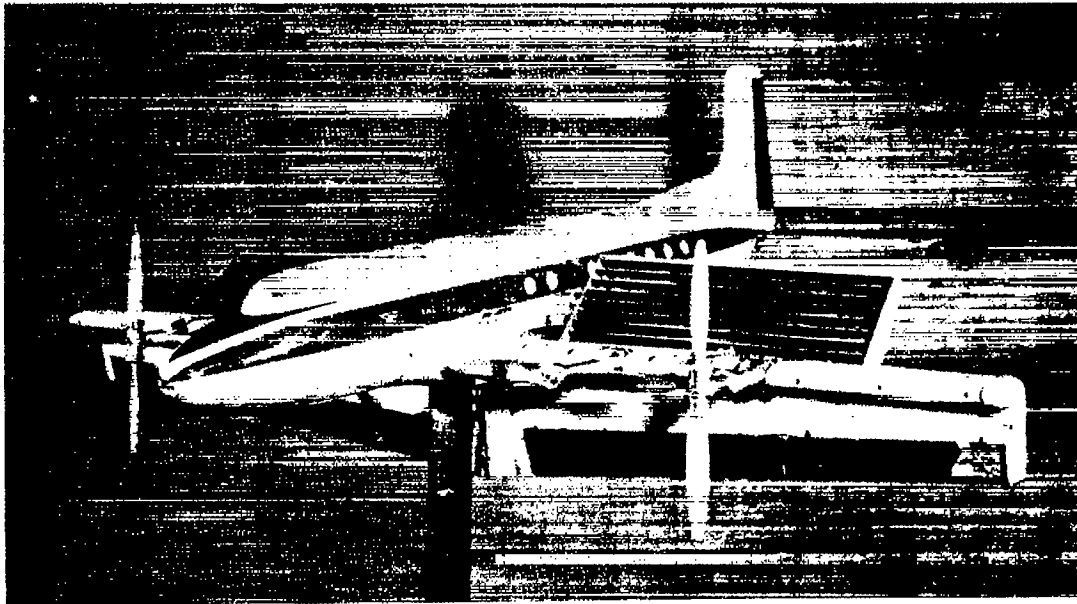


Figure 2.- Sketch of test setup for transition flights.



(a) Model in hovering configuration. L-93387



(b) Model in forward-flight configuration. L-93386

Figure 3.- Photographs of model in hovering and forward-flight configurations.

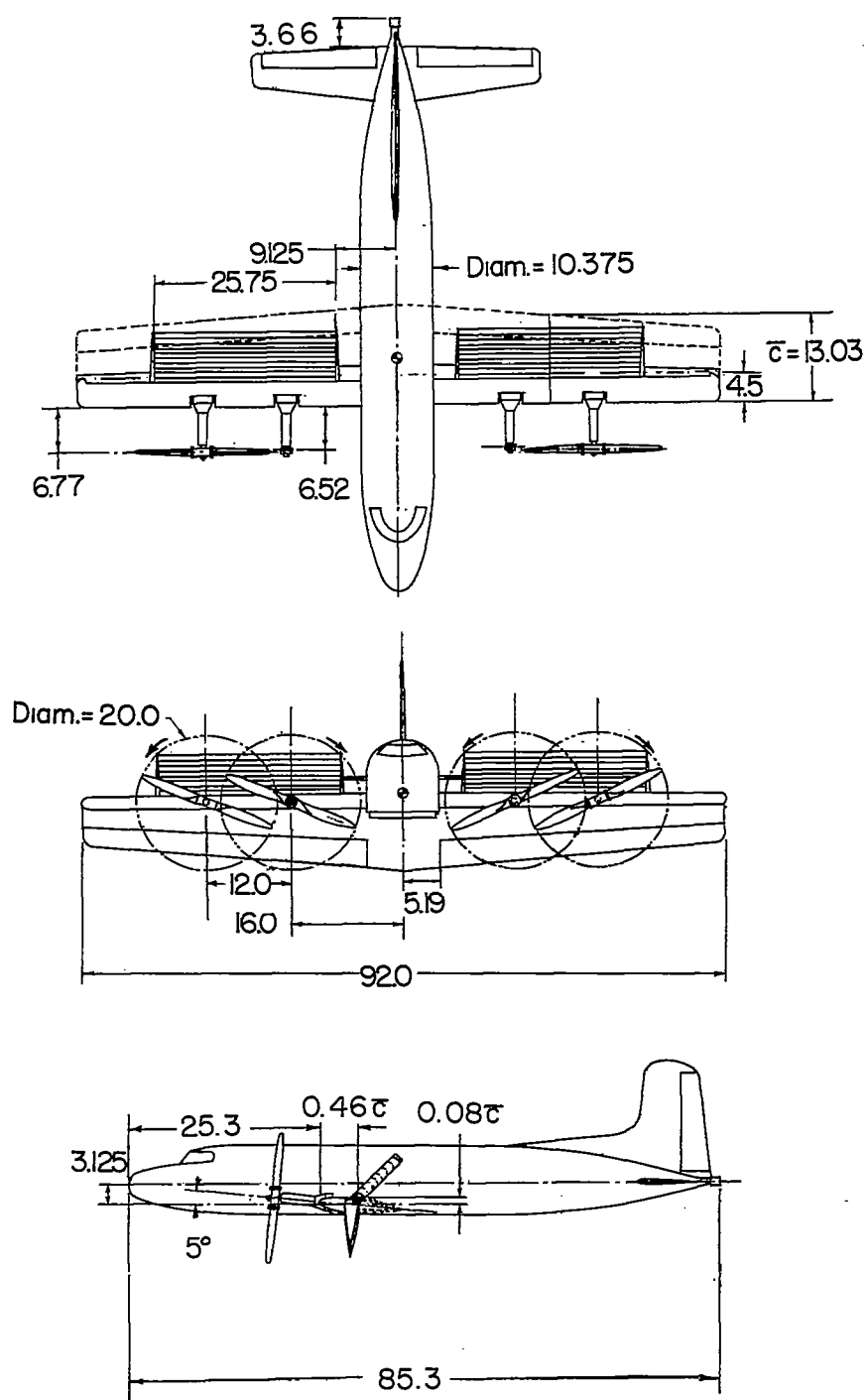


Figure 4.- Three-view sketch of model. All dimensions are in inches except as noted.

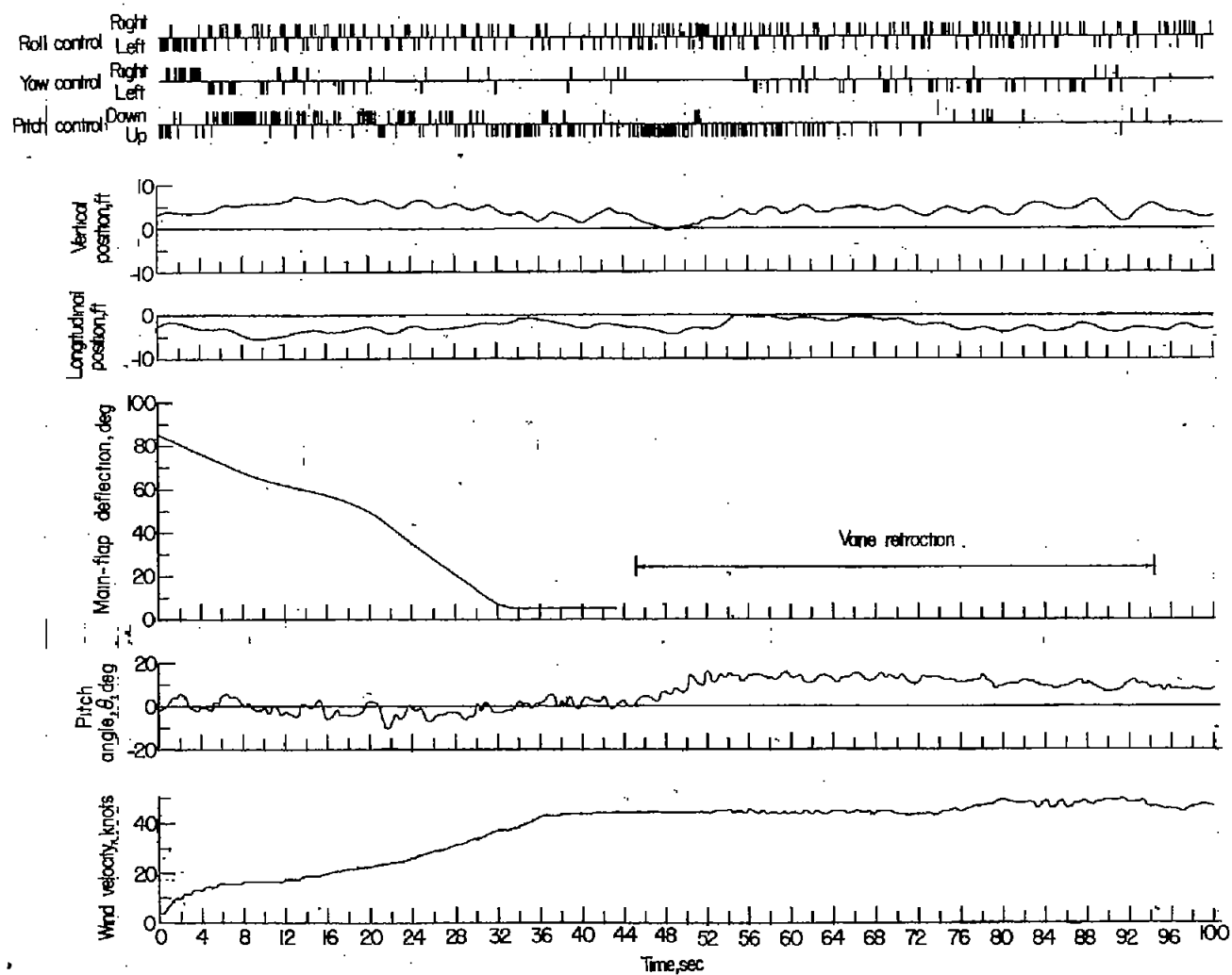


Figure 5.-- Time history of a transition flight. Center of gravity at 39 percent mean aerodynamic chord.

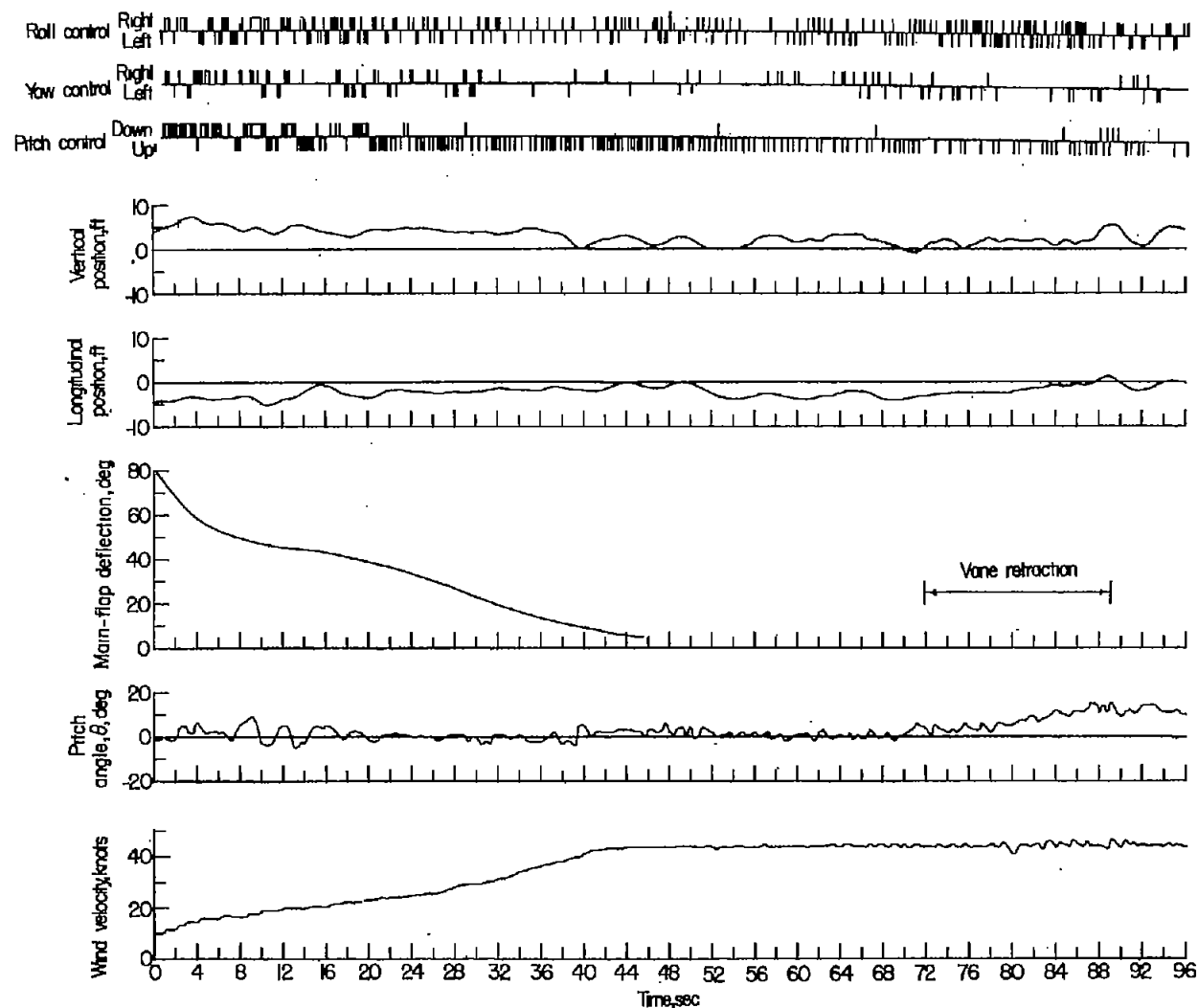


Figure 6.- Time history of a transition flight. Center of gravity at 46 percent mean aerodynamic chord.

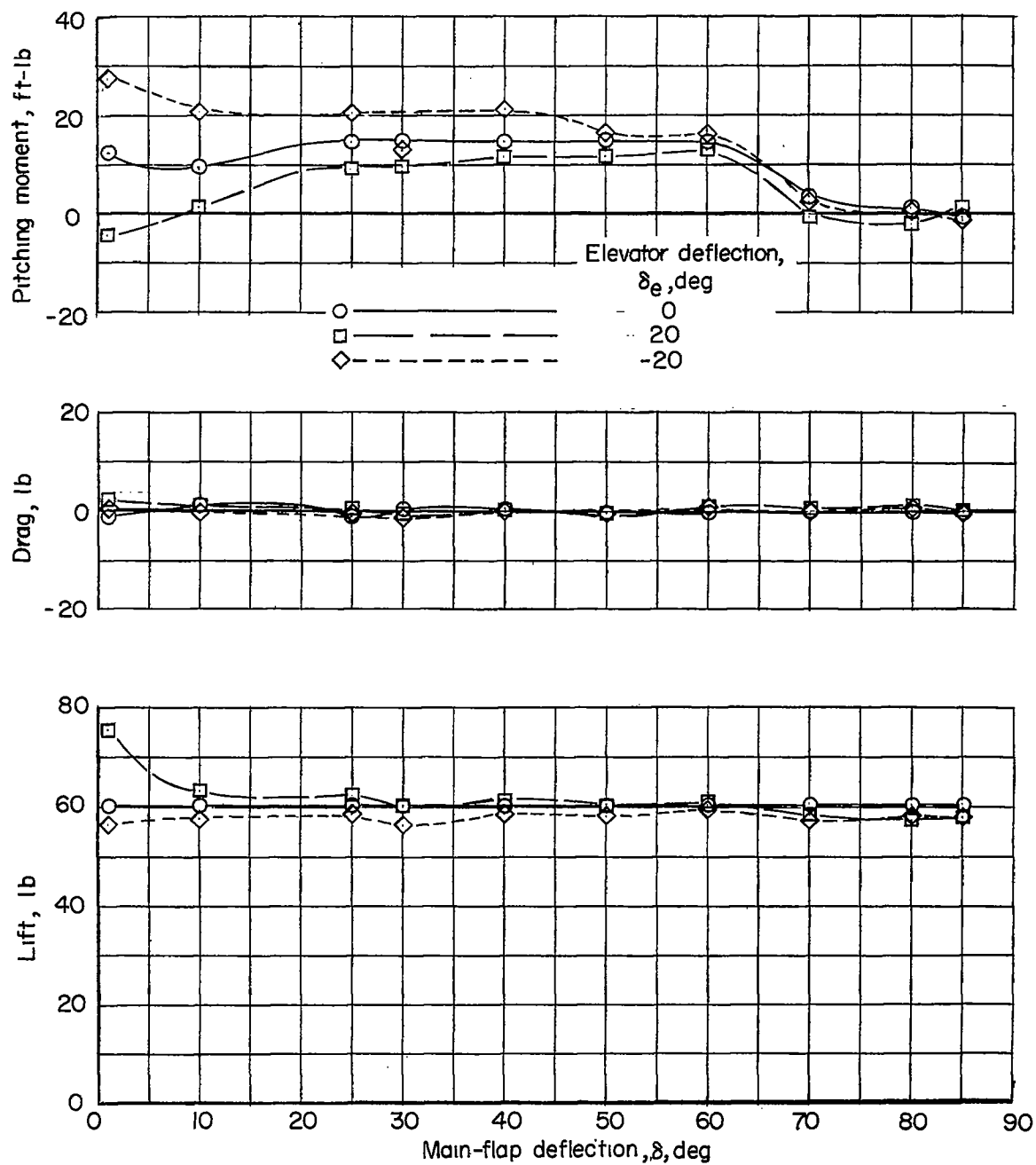


Figure 7.- Longitudinal control effectiveness obtained by use of elevator control with zero net drag when all controls are neutral.  
 $\beta = 0^\circ$ ;  $\alpha = 10^\circ$ .

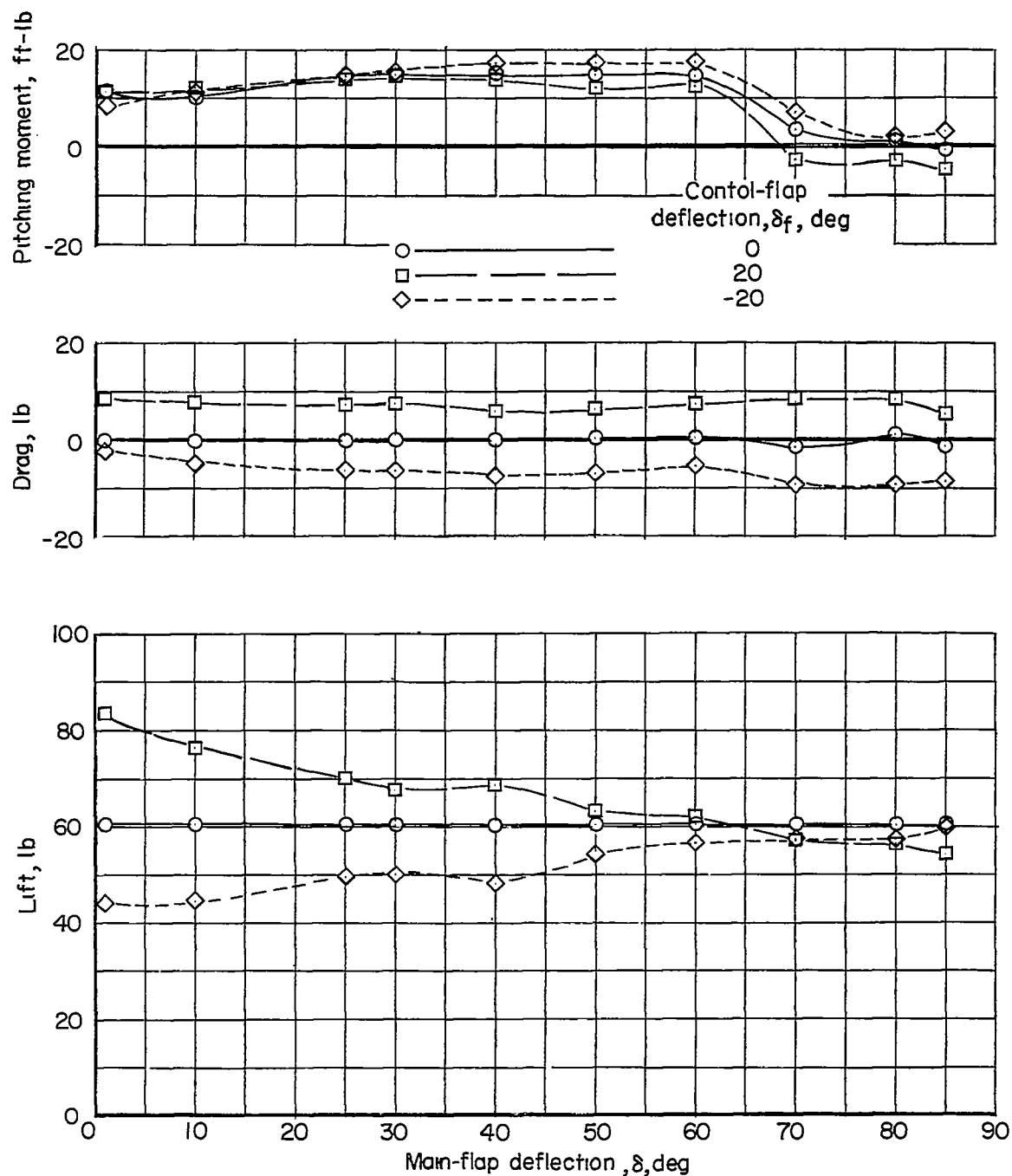


Figure 8.- Longitudinal control effectiveness obtained by use of the control flaps with zero net drag when all controls are neutral.  
 $\beta = 0^\circ$ ;  $\alpha = 10^\circ$ .



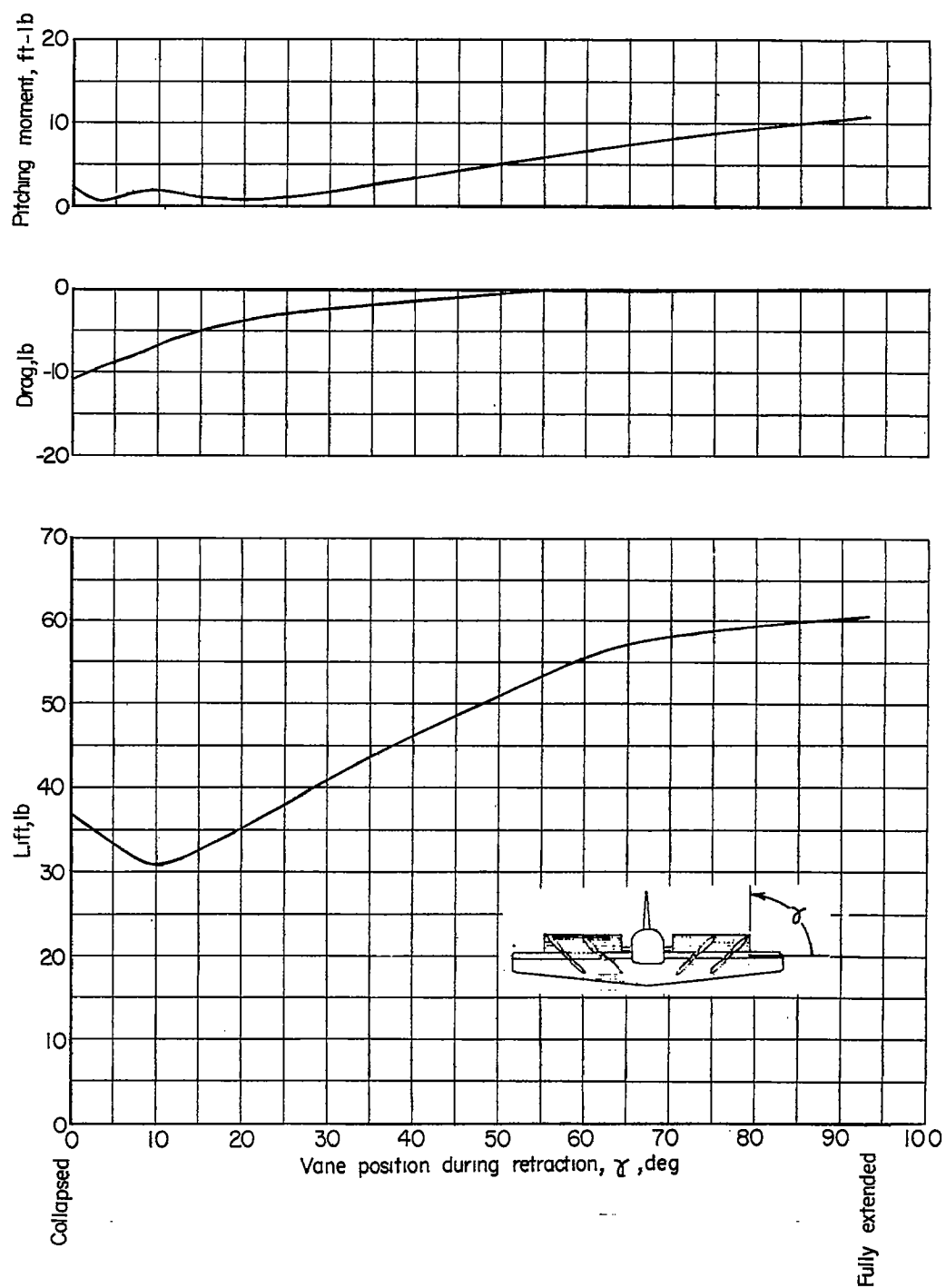


Figure 9.- Longitudinal characteristics of the model at various vane positions during retraction.  $\delta = 0^\circ$ ;  $\alpha = 10^\circ$ ;  $\beta = 0^\circ$ .

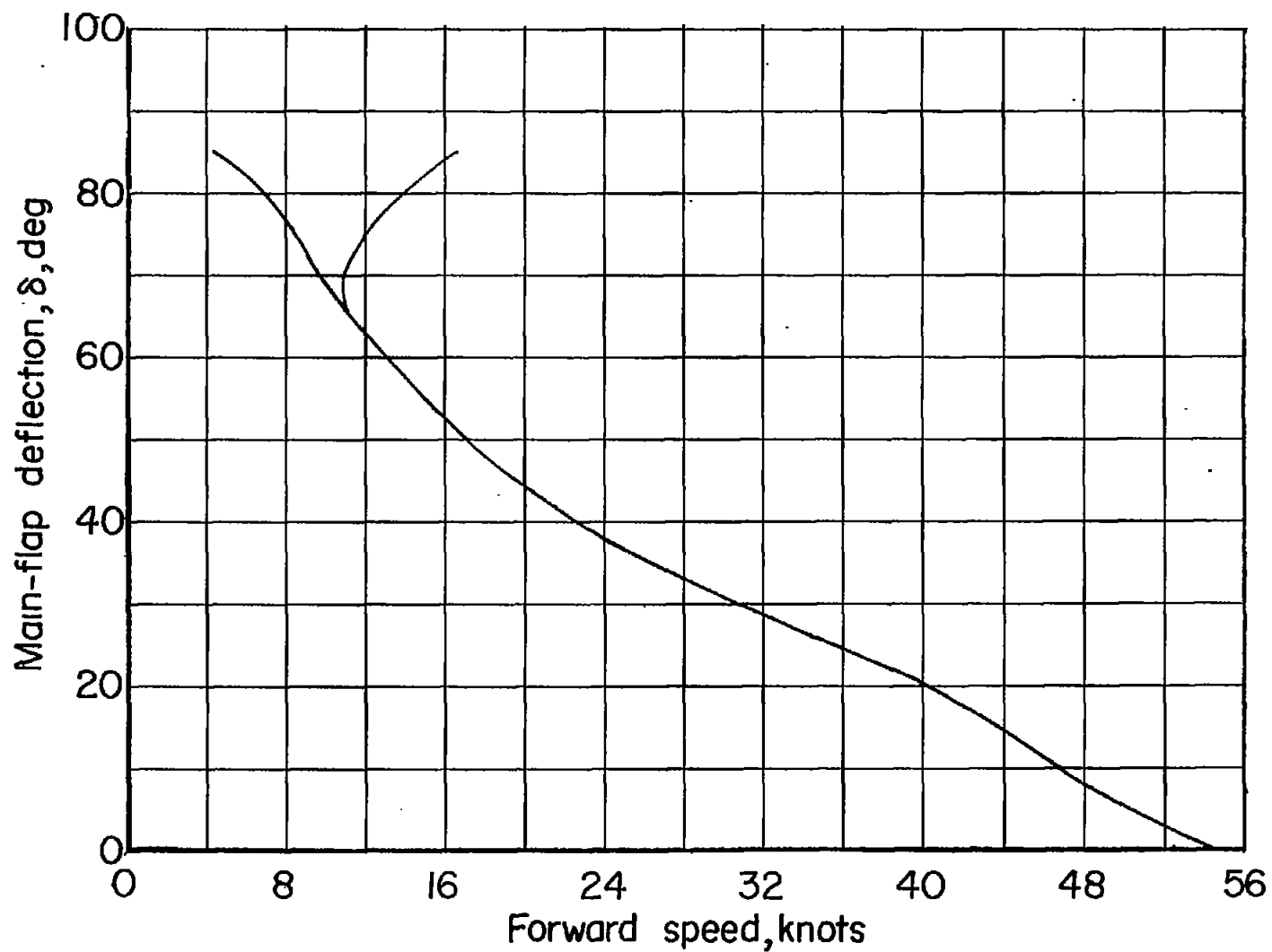


Figure 10.- Variation of main flap deflection with forward speed for steady level flight.  
 $\alpha = 10^\circ$ ; model weight = 60.5 pounds.

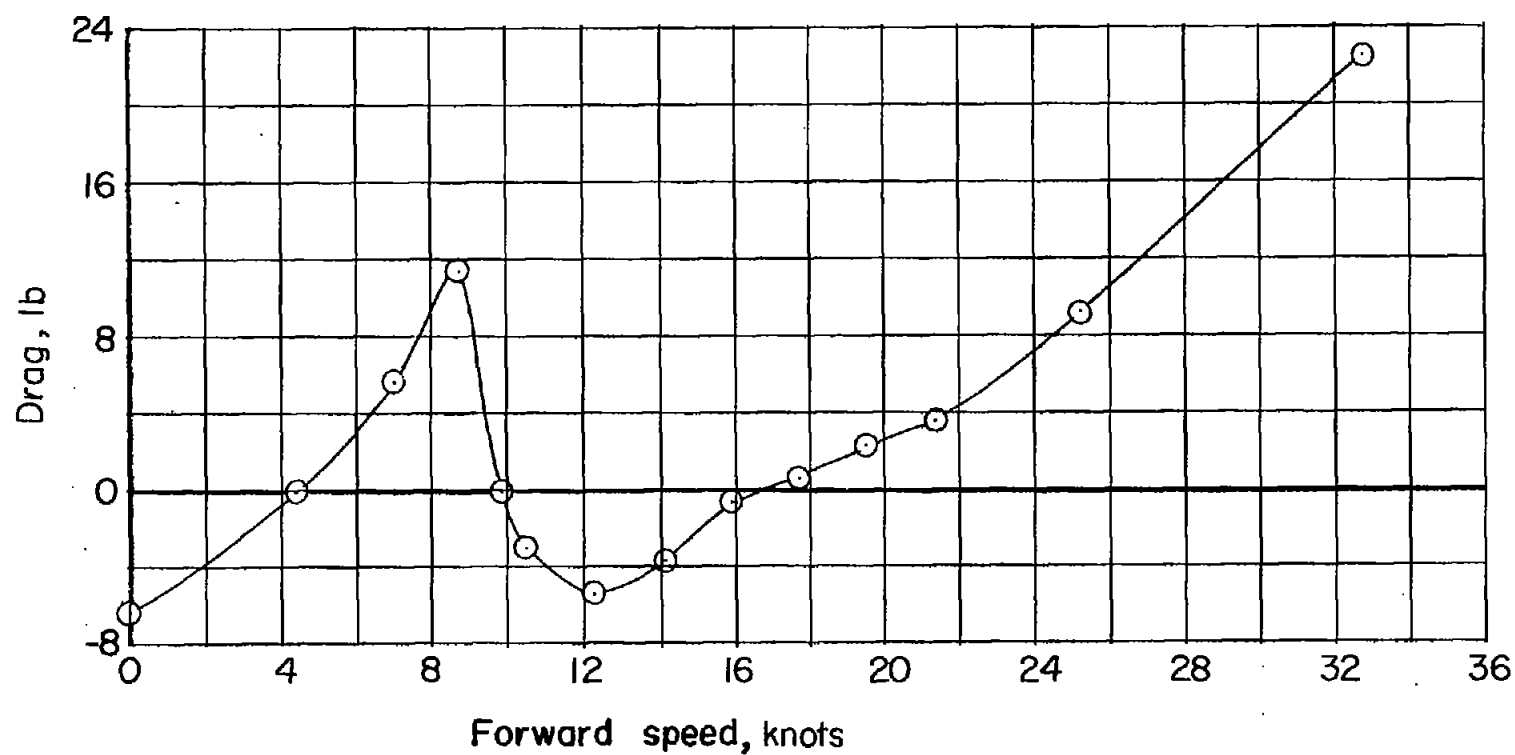


Figure 11.- Variation of model drag with forward speed.  $\delta = 85^\circ$ ;  $\alpha = 10^\circ$ ;  
model weight = 60.5 pounds.

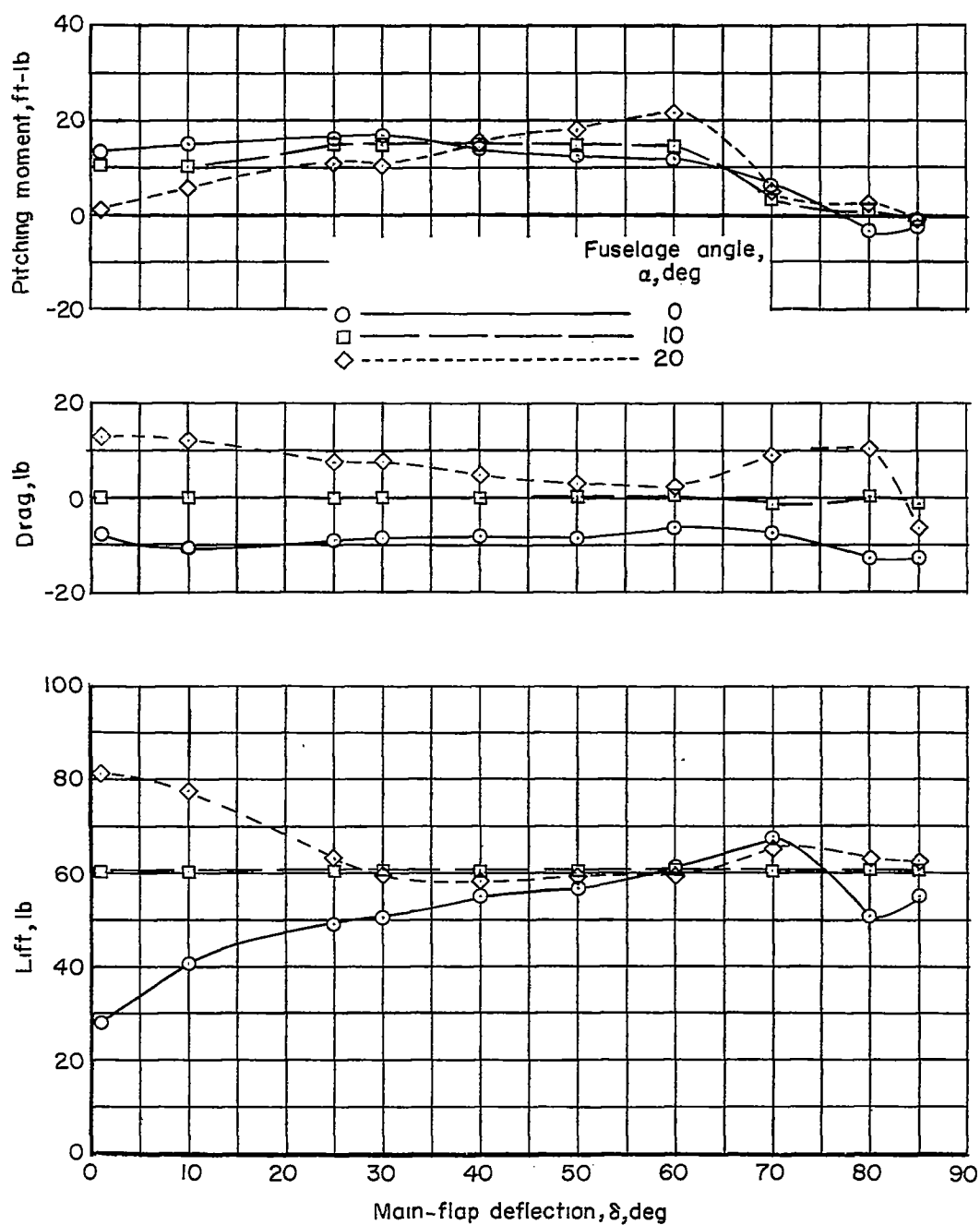


Figure 12.- Effect of fuselage angle of attack on aerodynamic characteristics in transition. Zero net drag when all controls are neutral and the fuselage at  $10^\circ$ .  $\beta = 0^\circ$ .

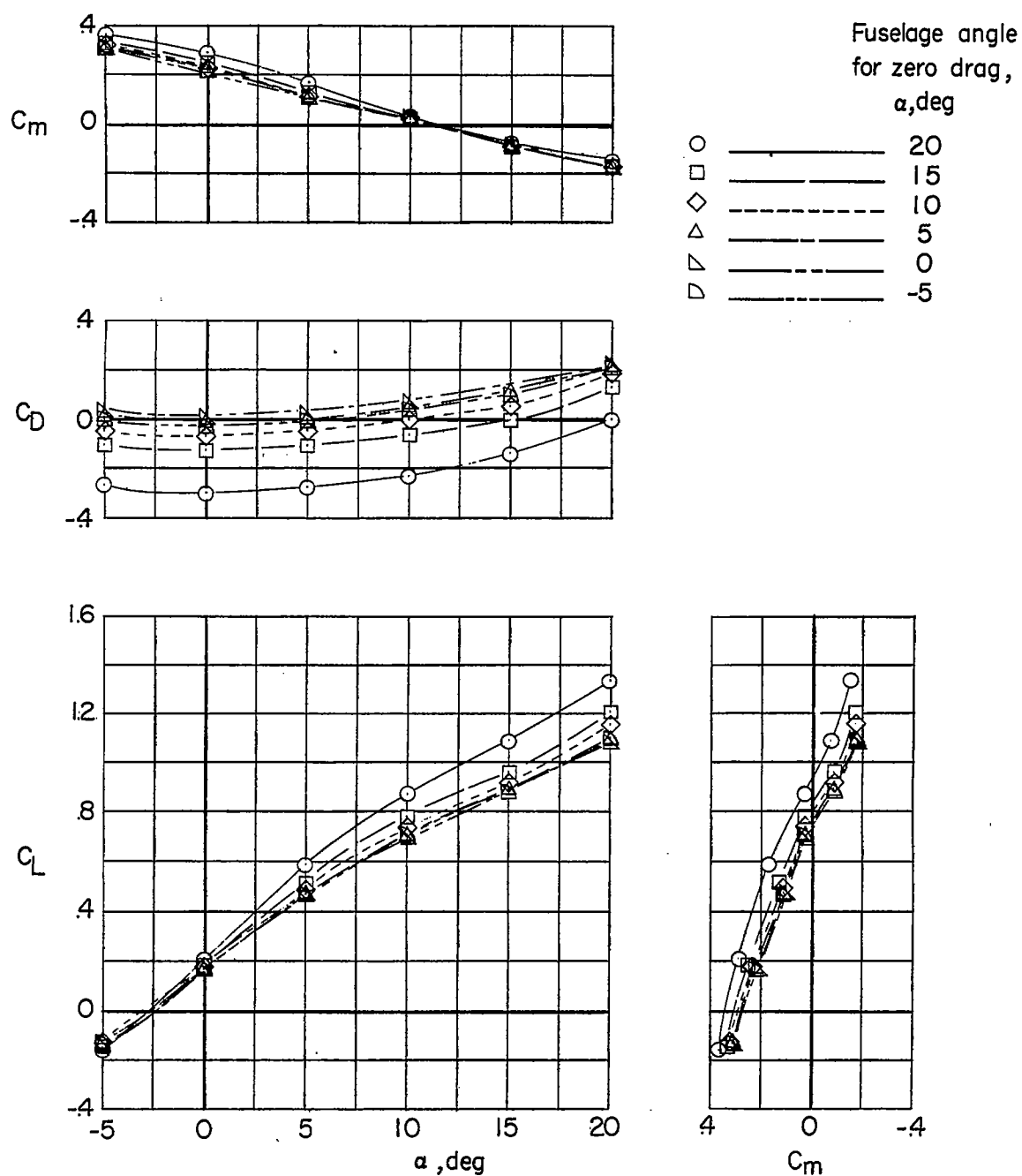


Figure 13.- Longitudinal stability characteristics for trim at various fuselage angles of attack. Power on; vanes retracted;  $\delta = 0^\circ$ ;  $\beta = 0^\circ$ .

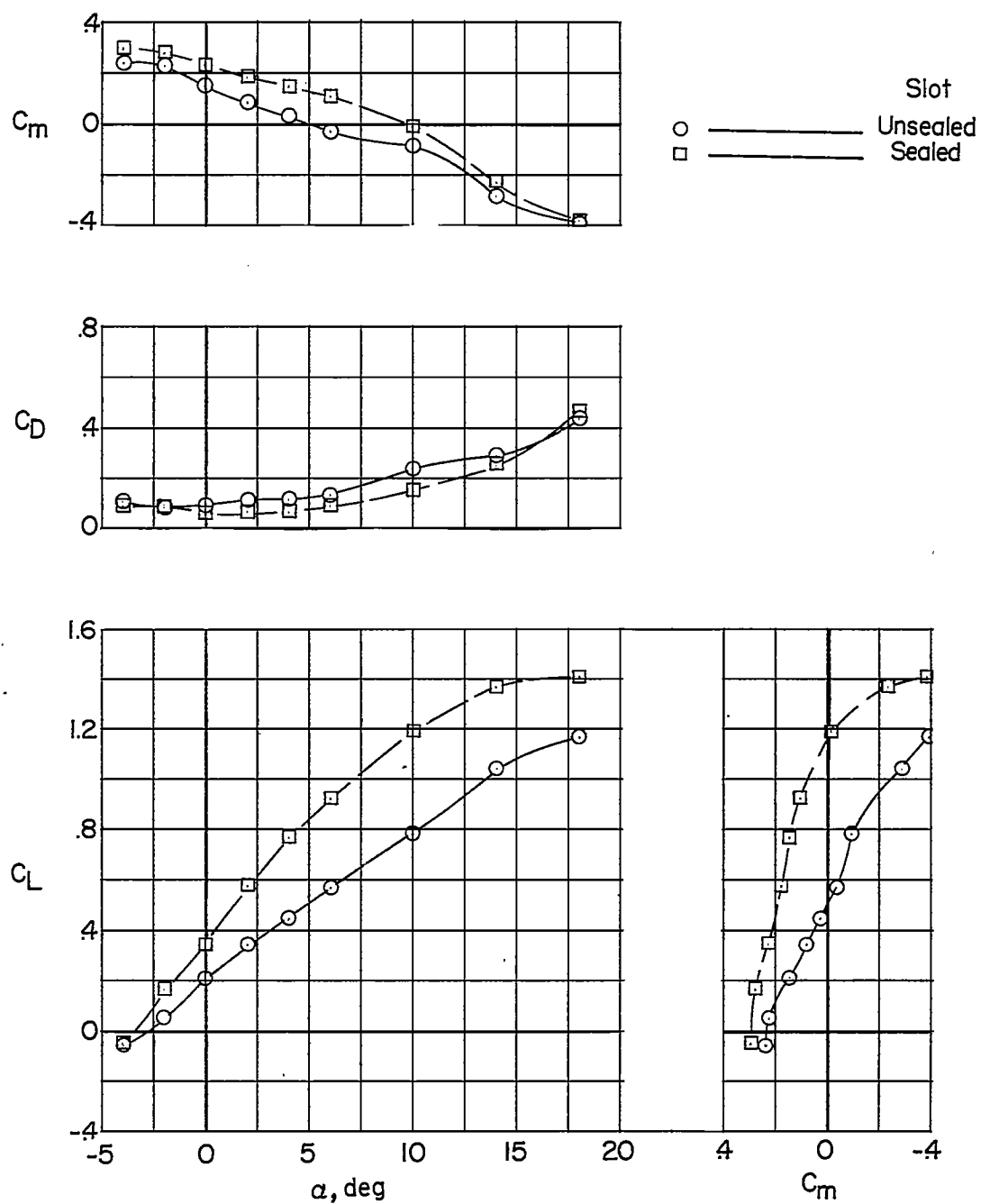


Figure 14.- Effect on aerodynamic characteristics of sealing slots for vanes in wing. All controls neutral; propellers removed; vanes retracted;  $\delta = 0^\circ$ ;  $\beta = 0^\circ$ .

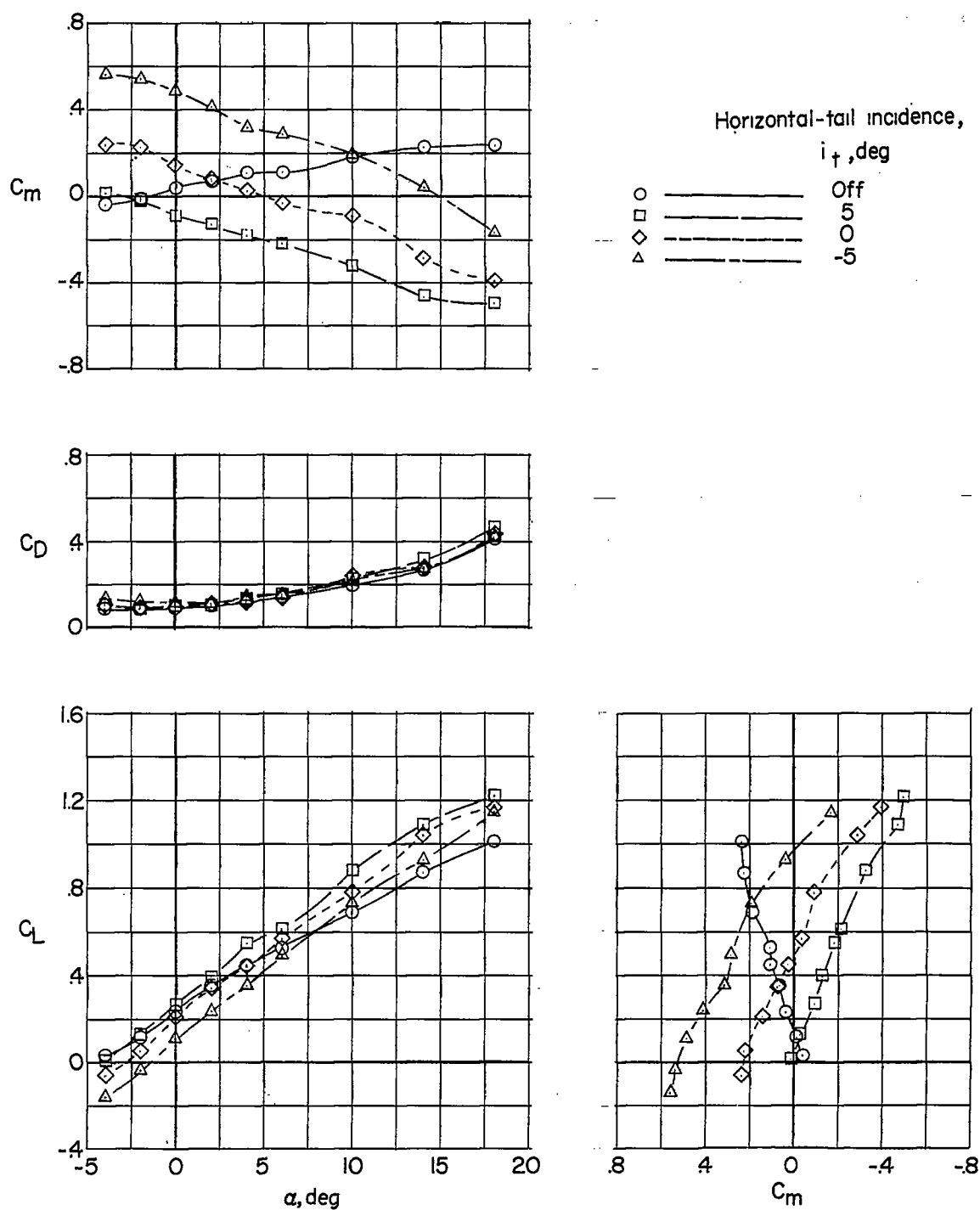


Figure 15.- Effect of horizontal tail incidence on aerodynamic characteristics. Propellers removed; vanes retracted;  $\delta = 0^\circ$ ;  $\beta = 0^\circ$ .

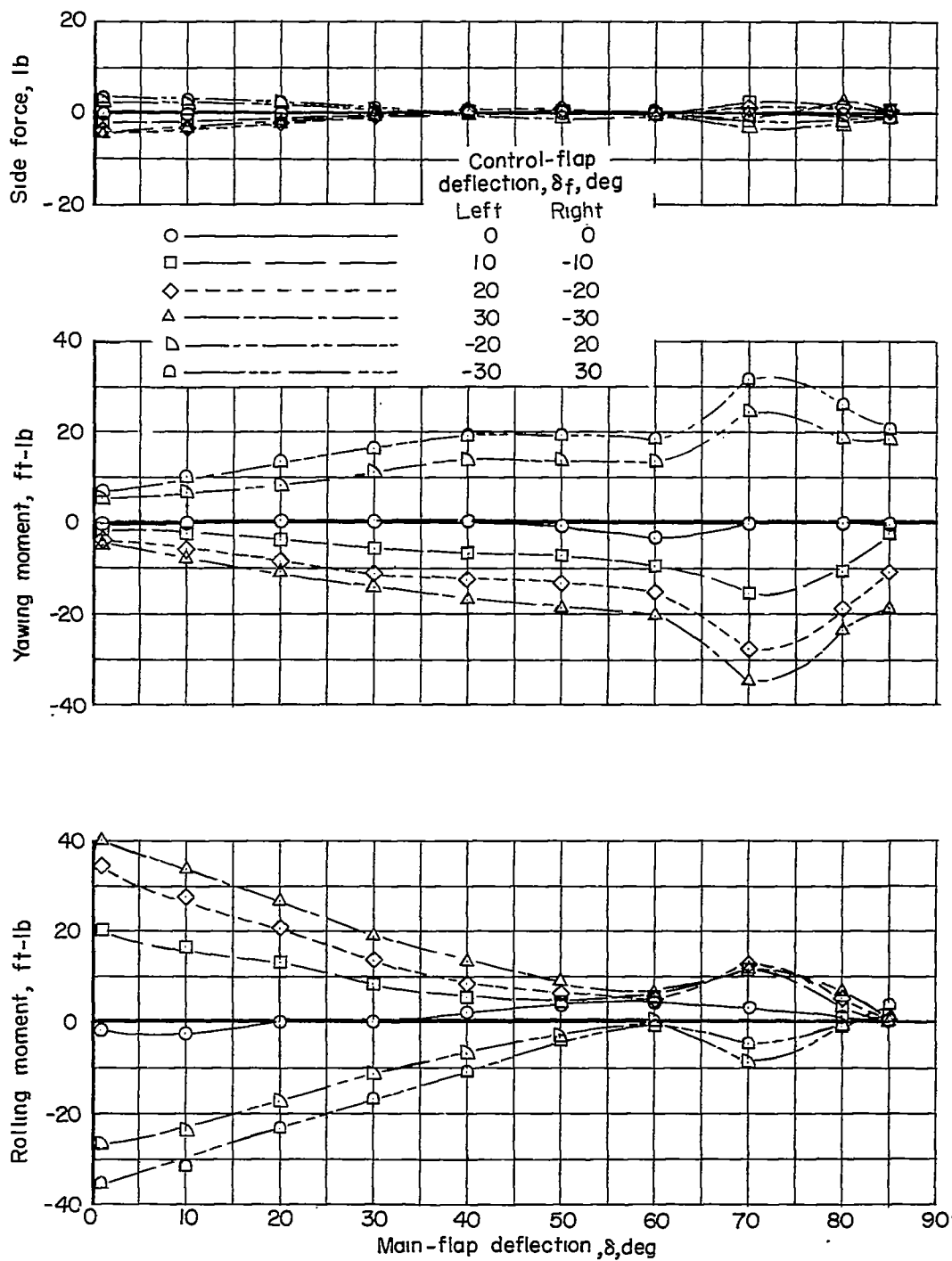


Figure 16.- Lateral and directional control effectiveness by use of differential wing control flap deflections for control with zero net drag when all controls are neutral.  $\beta = 0^\circ$ ;  $\alpha = 10^\circ$ .



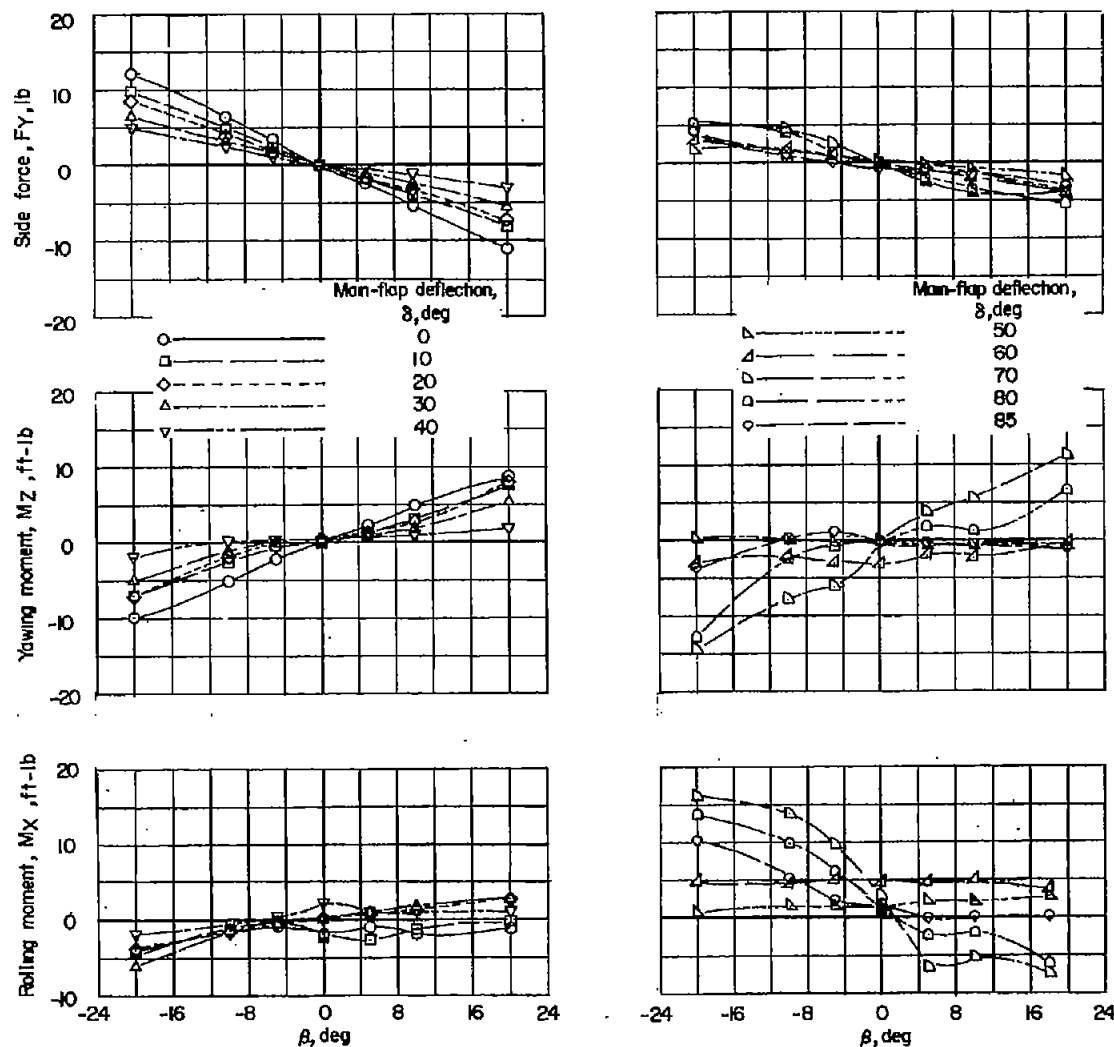


Figure 17.- Lateral characteristics of the model. All controls neutral; zero net drag at zero sideslip;  $\alpha = 10^\circ$ .

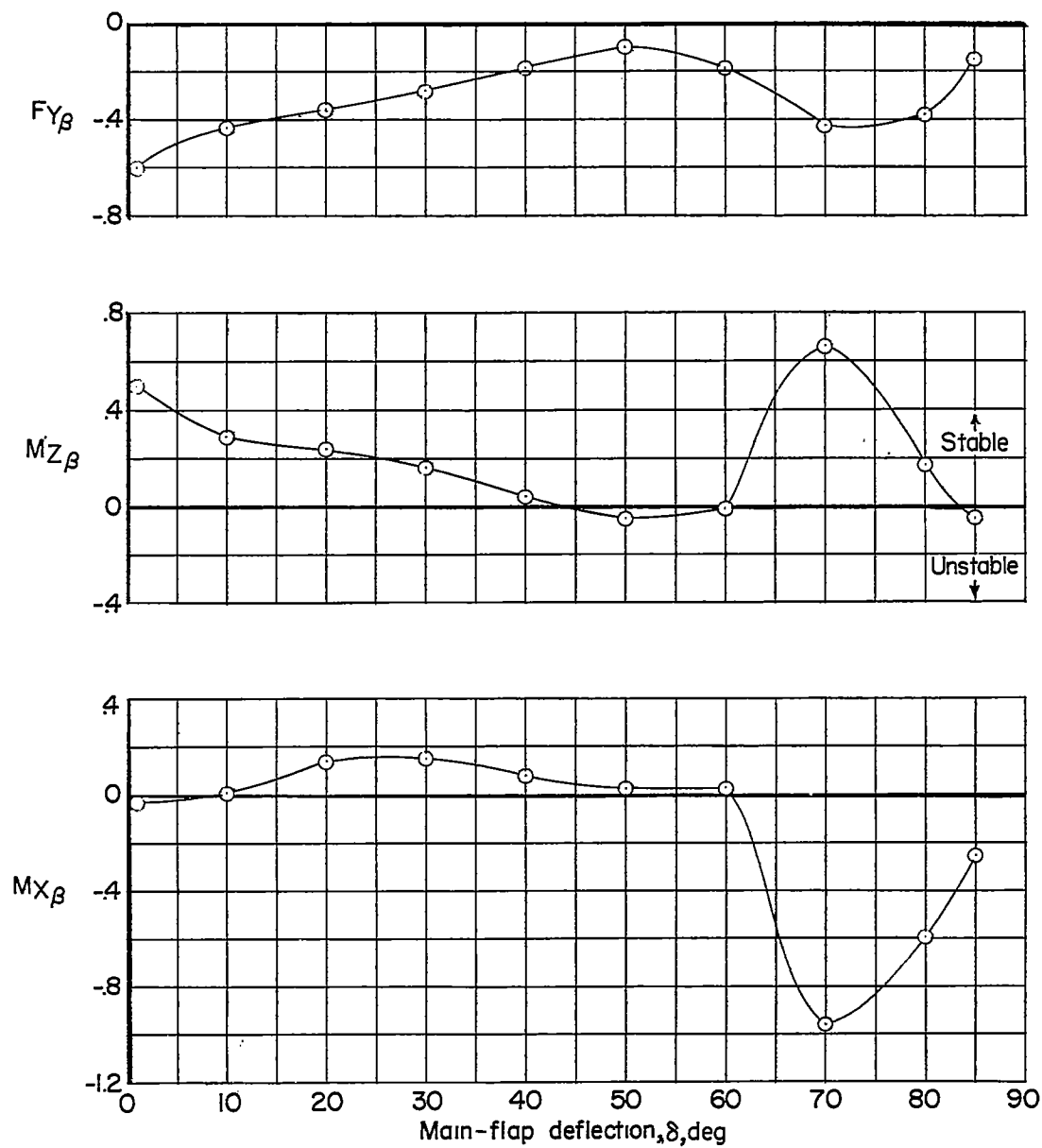


Figure 18.- Lateral stability characteristics of model. (Slopes taken for  $\beta$  between  $\pm 10^\circ$ .) Zero net drag at zero sideslip; all controls neutral;  $\alpha = 10^\circ$ .

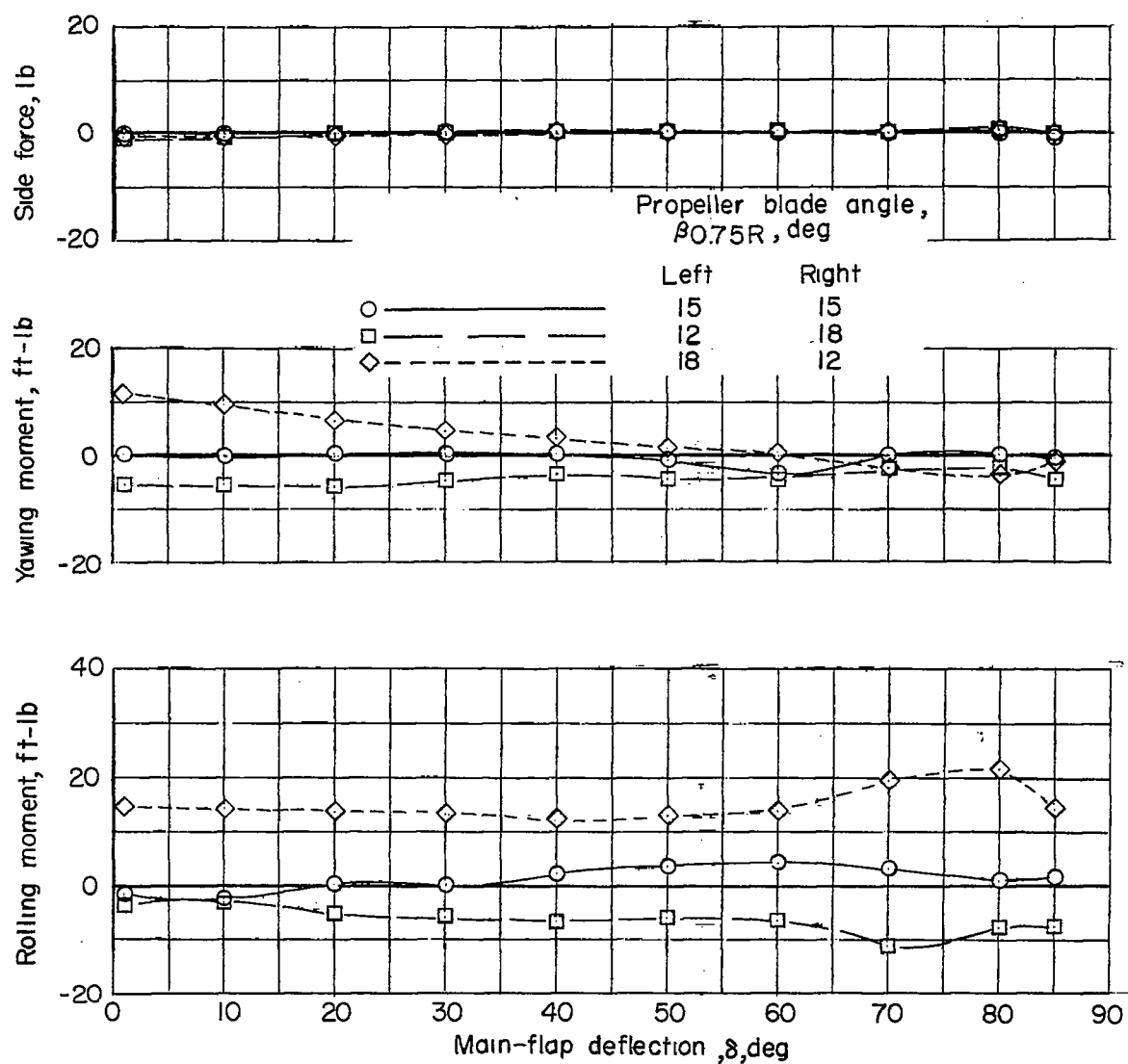


Figure 19.- Lateral and directional control effectiveness by use of differential variable-pitch outboard propellers for control with zero net drag when all controls are neutral.  $\beta = 0^\circ$ ;  $\alpha = 10^\circ$ .

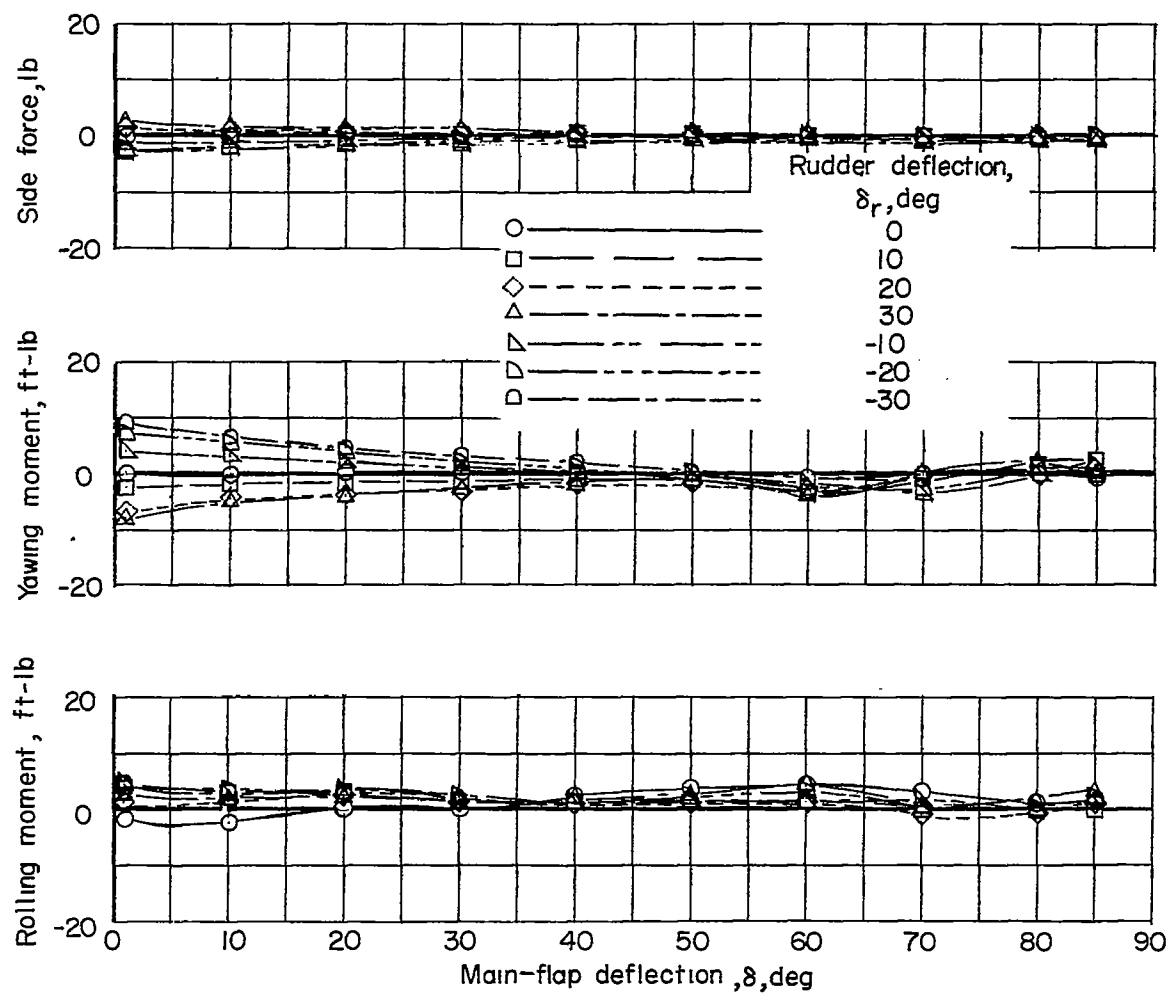


Figure 20.- Directional control effectiveness by use of the rudder control with zero net drag when all controls are neutral.  $\beta = 0^\circ$ ;  $\alpha = 10^\circ$ .

NACA TN 4131

A motion-picture film supplement is available on loan. Requests will be filled in the order received. You will be notified of the approximate date scheduled.

The film (16 mm, 3 min. 43 sec., color, silent) shows a closeup of the operation of the vanes retracting, a directional divergence, and transition flight tests of the model with the center-of-gravity positions at 39 and 46 percent mean aerodynamic chord.

Requests for the film should be addressed to the

Division of Research Information  
National Advisory Committee for Aeronautics  
1512 H Street, N. W.  
Washington 25, D. C.

CUT

Date \_\_\_\_\_

Please send, on loan, copy of film supplement to TN 4131

\_\_\_\_\_  
Name of organization

\_\_\_\_\_  
Street number

\_\_\_\_\_  
City and State

Attention Mr. \_\_\_\_\_

\_\_\_\_\_  
Title

Place  
stamp  
here

Chief, Division of Research Information  
National Advisory Committee for Aeronautics  
1512 H Street, N. W.  
Washington 25, D. C.